AIR ACCIDENTS
INVESTIGATION INSTITUTE
Beranových 130
199 00 Prague 9 – Letňany

CZ-23-0869

FINAL REPORT

on investigation of causes of an air accident of the PIK-20D glider,

**registration mark OM-5133,
in a field south of Podhořany near Ronov
on 12 August 2023**

Prague
February 2025

Contents

Abbreviations Used

AGL	Above ground level
AMSL	Above mean sea level
Cu	Cumulus
CHMI	Czech Hydrometeorological Institute
E	East
EASA	European Union Aviation Safety Agency
FAI	Fédération Aéronautique Internationale
LKPN	Public domestic airport Podhořany
FIR	Flight information region of Prague
METAR	Aviation routine weather report
MTOW	Maximum take-off weight
N	North
NIL None	
RADIO	Service providing information about known air traffic
RCC	Rescue Coordination Centre
REG QNH	Regional pressure, the lowest atmospheric pressure in the area (reduced to mean sea level according to standard atmospheric conditions)
RWY	Runway
ATCS	Air traffic control service
QNH	Atmospheric pressure in the area (reduced to mean sea level according to standard atmospheric conditions)
SCT	Scattered
SKC	Sky clear
SPL	Glider pilot licence
SYNOP	Report on surface synoptic observations made by weather stations
UTC	Coordinated Universal Time
AAII	Air Accidents Investigation Institute
VFR	Visual Flight Rules
VNL	Vision limitation
VRB	Variable

VZLÚ – National Center for Research, Development and Testing in Aerospace

Units Used

ft	Foot (unit of length – 0,3048 m)
hPa	Hectopascal (unit of atmospheric pressure)
kt	Knot (unit of speed – 1.852 km.h^{-1})

A) Introduction

Operator:	Natural person
Aircraft manufacturer:	Eiri Avion, Finland
Type of aircraft:	PIK-20D glider
Registration mark:	OM-5133
Location of incident:	800 m south-west of the LKPN RWY 07 threshold marks
Event date and time:	12 August 2023, 12:16 UTC (all times are UTC)

B) Synopsis

On 12 August 2023, the AAII was notified of an air accident of the PIK-20D glider on a field near the Podhořany airport. In the last third of the aerobatic sequence, the pilot made a right roll with transition to a half-loop. During the transition phase to the climb at approximately 500 m AGL, the left half of the wing broke off and the glider started rotating left around its longitudinal axis. This was followed by the spontaneous release of the right half of the wing and the fuselage started nose diving perpendicular to the ground.
The pilot jettisoned the cockpit canopy and left the glider cabin after unbuckling his seat belts. He immediately activated his emergency parachute, whose canopy was fully functional at approximately 200 m AGL. After a short parachute flight, he landed safely in a field near the wreckage of the glider's fuselage. The pilot was not hurt. The glider was completely destroyed in flight and also by the subsequent crash of the wreckage on the ground.
On the day of the accident, the AAII inspectors, in cooperation with the Police of the Czech Republic, started investigating the causes.

The cause of the incident was investigated by the Commission comprised of:

Commission Chairman:	Ing. Josef Bejdák
Commission member:	Karel Burger

The Final Report was issued by:

AIR ACCIDENTS INVESTIGATION INSTITUTE
Beranových 130
199 00 Prague 9 – Letňany

On 21 February 2025

This Final Report consists of the following main parts:

1 Factual Information
2 Analyses

1 Factual Information

The factual information was obtained from the testimony of the glider pilot, the chief judge of the competition day, by examining the wreckage, checking the glider documentation and meteorological information.

1.1 History of the Flight

1.1.1 Circumstances Preceding the Critical Flight

The pilot of the glider took part in the Podhořanský vejvraty 2023 aerobatic competition organised by the East Bohemian Aeroclub Pardubice, z.s. On Friday 11 August 2023, pilots were performing training flights since the morning. Saturday 12 August 2023 was reserved for the actual competition flights. Eleven pilots signed up for the competition. Out of these, eight were in the Sportsman category and three in the Intermediate category. The competition gliders included the ASK-21 glider borrowed from the Aero Club of the Czech Republic and the private PIK-20D glider. The Zlín Z-226 towing aircraft was used to tow the gliders. The competition was planned for both categories and for two rounds. After the first round, after 11 competition flights, the competition was terminated after the accident of the PIK-20D glider.

1.1.2 Critical Situation

The pilot carried out 6 out of 9 figures during the IAC Glider Sportsman 1 aerobatic sequence.
In the last third of the competition sequence, he made a right roll (figure 6) with transition to a half-loop (figure 7). During the transition phase to the climb at approximately 500 m AGL, the left half of the wing broke off and the glider started rotating left around its longitudinal axis. This was followed by the spontaneous release of the right half of the wing and the fuselage started nose diving perpendicular to the ground. The pilot jettisoned the cockpit canopy and left the glider cabin after unbuckling his seat belts. He immediately activated his emergency parachute, whose canopy was fully functional at approximately 200 m AGL. After a short parachute flight, he landed safely in a field near the wreckage of the glider's fuselage.

1.1.3 Statement of the Pilot

The pilot literally commented on the critical phase of the flight as follows: *"I have been flying figures 1, 2, 3, 4, and 5 from the competition sequence. After figure 6 (roll), I started to pull to figure 7. Immediately at the start of the pull, there was a bang and the glider started to shake violently. I estimate that at this point the nose of the glider was only about 10° above the horizon. I jettisoned the cockpit canopy. The glider began to rotate very quickly around its longitudinal axis. It took me a while to unbuckle my seatbelts, about 3 seconds, because the centrifugal force was pulling me hard out. After overcoming the resistance in the seatbelt lock, I flew out. I pulled the handle of the parachute with my right hand and it opened very quickly. At that moment, about 30 to 40 metres from me, a wingless fuselage flew by, falling perpendicular to the ground. Using the controls, I turned the parachute into wind and landed in a field about 30 meters from the fuselage without any injury. I estimate the altitude at the* *time of the glider's destruction to be about 500 m AGL. The parachute opening altitude was about 200 m AGL."*

In a subsequent interview, the pilot told the Commission: *"I was quite familiar with the handling of the seat belts, as there are the same seat belts in ASK-21. But I was surprised by the great force required to turn and unlock the lock, caused by a large negative overload."*

1.1.4 Witnesses' Statements

In his testimony, a witness, the chief judge, stated, inter alia: *"The aero-tow of the PIK-20 glider into the aerobatic box was carried out in the normal manner with the approach from the east in the direction of runway 25. In a standard manner, the glider was given radio clearance by the chief judge to enter the aerobatic box and at the start of the aerobatic sequence, the box was free. The glider disconnected approximately 500 metres east of the aerobatic box at an altitude of approximately 1,300 m AGL. The glider flew into the aerobatic box and started the competition flight by flapping its wings and then performed the aerobatic competition figures 1, 2, 3, 4, and 5 from the Sportsman 1 aerobatic sequence (see Appendix IAC Glider Sportsman Known 1 with the left wing destruction point marked with a red cross). After he completed figure 6 (roll), the left wing was destroyed immediately after this figure at an altitude of 400–500 m AGL. The glider entered a left spiral dive after the left wing separation and continued in this position almost perpendicular to the ground. After about 2 to 3 seconds after the destruction of the left wing of the glider, when the parachute canopy was not visible yet, I clearly and distinctly instructed the pilot via RADIO Podhořany on the frequency 123.590 MHz with the words: "Jump out! Jump out!" In about 1 second the parachute canopy appeared in the sky near the falling wreckage and the wreckage narrowly missed the pilot on the parachute without any signs of collision with him or the parachute. I estimate the altitude of the canopy opening to be about 100 m above the level of the Podhořany airport, probably about 200 m above the place of impact of the wreckage and the pilot to the west in the extension of runway 25. About 5 minutes after the accident, I received a phone call that the pilot of the glider was OK."*

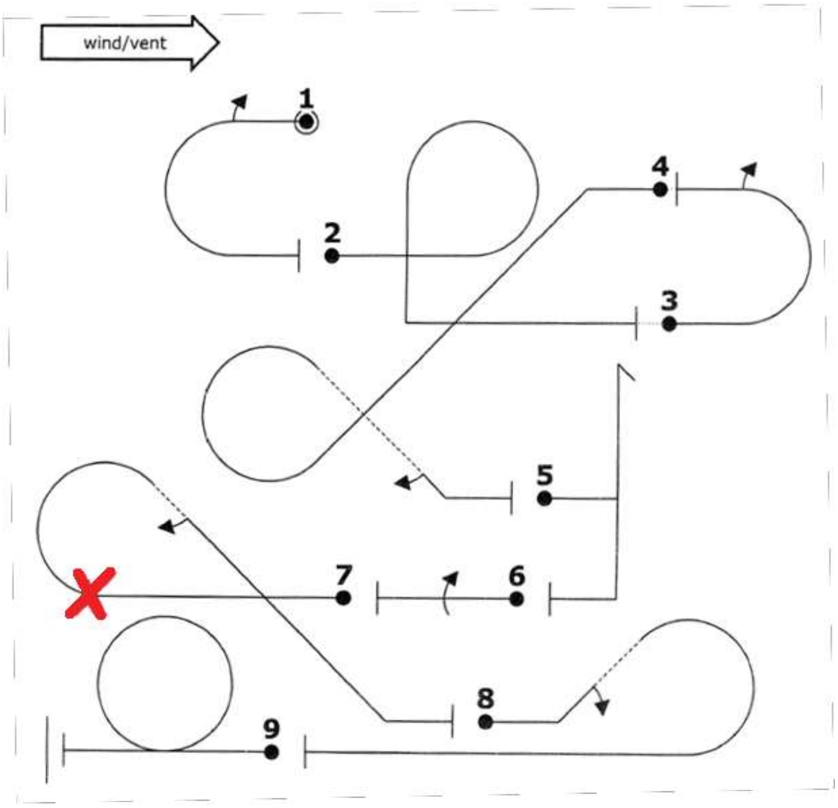

Fig. 1 – Scan of the aerobatic sequence *IAC Glider Sportsman Known 1*

1.2 Injuries to Persons

The pilot did not suffer any injuries during the accident. The Police of the Czech Republic carried out an orientation breath test using the Dräger tester with a negative result.

Table 1 – Personal injuries

Injuries	Crew	Passengers	Other persons (inhabitants, etc.)
Fatal	0	0	0
Serious	0	0	0
Light/No injury	0/1	0/0	0/0

1.3 Damage to Aircraft

The glider was completely destroyed in flight and also by the subsequent crash on the ground.

1.4 Other Damage

There was no further damage at the accident site. The individual parts of the glider did not cause any damage to the third party property when hitting the ground in the municipality of Podhořany near Ronov.

1.5 Personnel Information

The pilot, aged 54 years, holder of a valid flight crew licence / SPL, aerobatics-s rating. He held a valid class 2 medical certificate with VNL limitation, and a valid licence of the aeronautical mobile service radio operator. The weight of the pilot with the parachute was about 85 kg.

According to the data in the flight logbook, he has flown gliders of various types (BF-3, L-13A, L-23, VT 116, L-13AC, GROB G-102 ASTIR CS, M-28, M-35, LG-125, SG-38, GRUNAV BABY II.b, STANDARD CIRRUS, Z-24 KRAJÁNEK, K-6E, LF-107 LUŇÁK, ASK-21, PIK-20D) and has performed 320 flights, totalling 188 hrs 54 min, since 2012. He obtained aerobatics-s rating for advanced flying of gliders on 14 October 2019. In aerobatics, he has flown a total of 14 hrs 38 min and has performed 62 flights.

In 2023, he flew only the PIK-20D type and carried out 5 flights lasting 4 hrs 55 min, out of which 4 aerobatic ones amounting to 55 min. On the day of the critical flight, the pilot made one approximately 10-minute flight with the PIK-20D glider. It was the last competition sequence of the first round. The pilot placed sixth in his category despite not completing the competition flight.

1.6 Aircraft Information

1.6.1 Technical Description

The PIK-20 competition glider was designed in response to the changed conditions for the FAI standard class after water ballast, retractable landing gear, and flaps coupled with aerodynamic brakes were allowed for this category. The project was developed by the Department of Aerospace Engineering at the University of Helsinki (the abbreviation PIK was derived from Polyteknikkojen Ilmailukerho – university aeroclub). The prototype was flown on 10 October 1973.

The glider design was continuously improved during manufacture. The wing mechanism was modified and carbon wing spars were introduced during production of the B version. The PIK-20B thus became the first mass-produced glider to use carbon composite as a construction material.

In 1975, again in close cooperation between Eiri Avion and the University of Helsinki, the development of a completely new version was started. The first flight of the prototype version D took place on 19 April 1976. A major change was the re-engineering of the wing mechanism with the use of Schempp-Hirth style retractable aerodynamic brakes. The critical areas of the fuselage were reinforced with carbon strips and some parts were made of carbon composites. Approximately 162 units were manufactured, including the version D-78 produced since 1978.

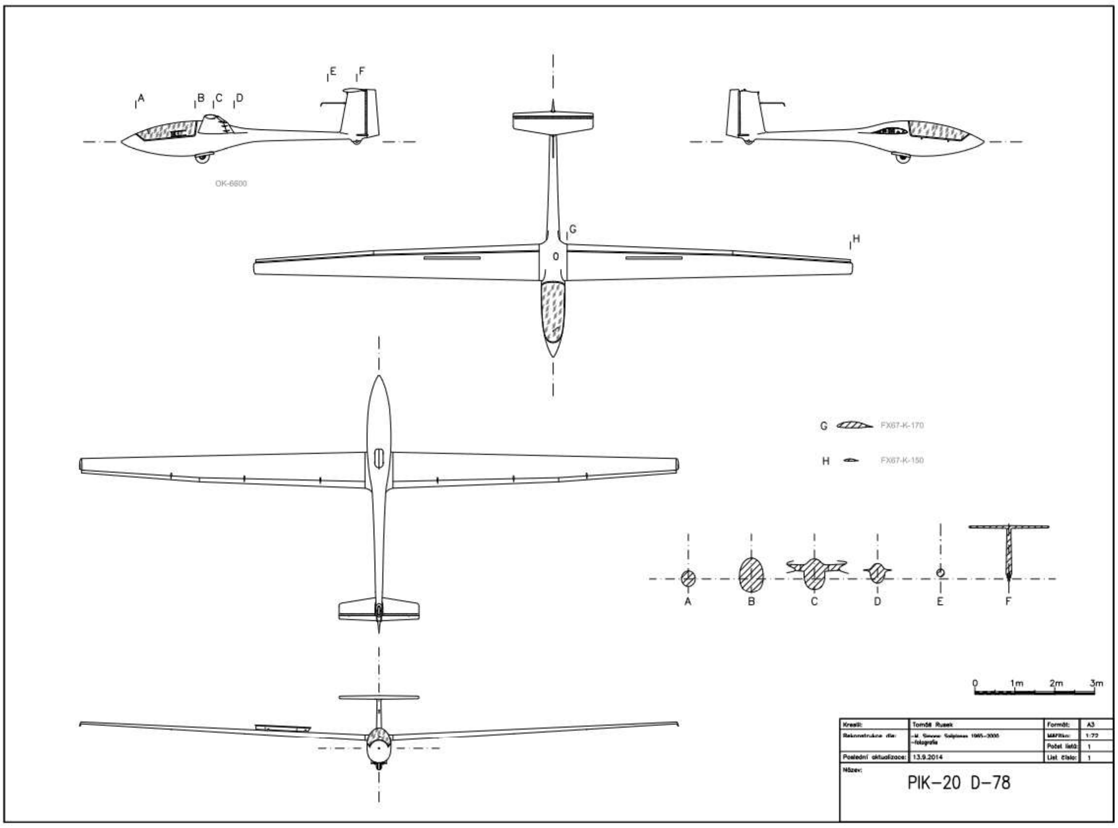

Fig. 2 – Scan of the technical drawing of the PIK-20D-78 glider

1.6.1.1 Wing

Description of the wing design:

The wing is tapered, self-supporting, single-spar, divided in the middle. It has a shell construction, consisting of a fibreglass sandwich with a 10 mm thick layer of Lynizel PVC foam. The wingtips are finished with end bows that are deflected downwards. There is Wortmann FX 67-K-170 profile at the wing root and the FX 67-K-150 profile at wingtips. Wing dihedral angle is 3°. The root chord is 0.9 m, the mean chord is 0.65 m and the tip chord is 0.36 m.

The ailerons and flaps have a sandwich construction with 3mm PVC foam filling. The axis of rotation of the flaps is in the middle of the profile in the D version and there are elastic transitions between the flap and the aileron. The ailerons are extended to the wingtips. The flaps and ailerons are linked, but the new feature is the dependence of the flap on the aileron deflection, so the whole works as a flaperon. In addition, when the flaps are deflected, the longitudinal balance is automatically adjusted. Schempp-Hirth brake flaps are installed on the wing and extend from the upper surface of the wing.

The spar has a rectangular cross-section and consists of a full length upper and lower flange made of carbon composite and a web made of laminated long-fibre unidirectional fibreglass.

Mutual connection of both wing halves:

The connecting element of both wing halves is a steel connecting pin. The end of the spar protruding from each wing half, called the spar stub, is inserted into a rectangular hole in the fuselage during assembly. Both spar stubs are adjacent to each other in the fuselage. The relative position is secured by a connecting pin, which is inserted into the bushings in the spar stubs. The connecting pin is secured by a safety pin.

The locking elements for the correct installation position of the wing are two (front and rear) ball bushings located on the left side of the fuselage and two (front and rear) ball bushings located on the right side of the fuselage. The two (front and rear) guide pins of the left wing half are inserted into the bushings on the left side of the fuselage during assembly. The two (front and rear) guide pins of the right wing half are inserted into the bushings on the right side of the fuselage during assembly. The guide pin of the left wing spar is inserted into the bushing located in the root rib of the right wing side during assembly. The guide pin of the right wing spar is inserted into the bushing located in the root rib of the left wing side during assembly.

1.6.1.2 Tailplanes

The tailplanes are T-shaped. The rudder and elevator are made as a fibreglass shell with a PVC foam sandwich.

1.6.1.3 Fuselage

It is made as a laminate shell stiffened with eight ribs. Its height is 0.86 m and its width is 0.6 m. The 3mm plexiglass cockpit canopy opens to the right and can be jettisoned in an emergency. In the closed position, it is sealed with a hose that is pressurised by a balloon pump. The foot pedals are adjustable with pull rods. The instrument panel stand is installed in front of the pilot on the floor. On the left side of the cockpit, there are two levers – black one for flap control and blue one for the aerodynamic brakes. The tow rope release rod is located on the left side of the cockpit next to the instrument panel. On the left side of the cockpit, there is also a green spring trim control. On the right side of the cockpit, there is a landing gear control lever. The landing wheel is braked via a lever located on the control lever. The main retractable landing wheel is unsprung and equipped with a drum brake. It is covered with a two-piece door in the retracted position. A fixed tailwheel is located under the rear fuselage. The total pressure sensor is fitted in the tip of the fuselage, the static pressure sensors are placed on the sides of the middle part of the fuselage. The pressure sensor for the variometer is in the fin surface. The tow rope attachment is located in the lower part of the fuselage in front of the landing gear bay. There is a water ballast tank discharge valve behind the landing gear bay. The water tanks can hold max. 140 kg of water.

1.6.2 General and Performance Characteristics

General Characteristics:

- Crew 1
- Length 6.43 m
- Span 15.0 m
- Height 1.34 m
- Wing area 10.0 m^2
- Wing surface load 45.0 $kg \cdot m^{-2}$ (with water ballast)
- Empty weight 225 ±6 kg
- MTOW for aerobatics 360 kg

1.III **Technical Characteristics and Operational Limitations**

Model PIK-20D, Approved September 21,1976

Serial Nos.	20504 and up		
Maximum Weight	450 kg (990 lbs) including water ballast		
Water Ballast	Two water ballast tanks at station 2130 mm (83.9 in) each 70 kg (154 lbs)		

Control Surface Movements

		Up	Down
Flaps		12° ± 1°	16° ± 1°
Ailerons	+16° flap	$13^{\circ}{}^{+2^{\circ}}_{-1^{\circ}}$	$12{,}5^{\circ}{}^{+2^{\circ}}_{-1^{\circ}}$
	0° flap	$12^{\circ}{}^{+2^{\circ}}_{-1^{\circ}}$	$11^{\circ}{}^{+2^{\circ}}_{-1^{\circ}}$
	-12° flap	$11^{\circ}{}^{+2^{\circ}}_{-1^{\circ}}$	$9{,}5^{\circ}{}^{+2^{\circ}}_{-1^{\circ}}$

Aileron neutral position travels with flaps up 12° ±1° thru down 16° ±1°

Elevator	Up 20° ± 1°	Down 20° ± 1°
Rudder	Right 33° ± 2°	Left 33° ± 2°

Fig. 4 – Scan EASA.SAS.A.024 Issue 05, 27/08/2021 PIK-20D Page 2 of 10

1.6.3 Performance

- Max. design speed V_{NE} — 292 km·h^{-1}
- Max. speed with flaps V_F — 150 km·h^{-1}
- Max. speed in turbulence V_{VB} — 200 km h^{-1}
- Manoeuvring speed V_A — 190 km·h^{-1}
- Max. aero-towing speed V_T — 190 km·h^{-1}
- Winch launch speed W_W — 125 km·h^{-1}
- Stall speed V_{SI} — 60–74 km·h^{-1} (flaps 16°)
- Gliding ratio — 1:38 – 1:42
- Permissible load factors — +6.6/-4.6 g (without water ballast)

1.6.4 Crashed glider

- Type of glider — PIK-20D
- Manufacturer — Eiri Avion, Finland
- Serial number — 20559
- Registration mark — OM-5133
- Year of manufacture — 1977
- Empty weight (last weighing report) — 243 kg
- Total hours flown — 4 555 hrs 47 min
- Number of launches — 1,484
- Hours flown since the last inspection — 4 hrs 55 min
- Launches since last inspection — 5
- Statutory insurance: — valid

Fig. 5 – Glider PIK-20D, registration mark OM-5133

1.6.4.1 Glider operation

The glider was sold from the factory to Austria, where it was operated by a private owner in a shared mode until 2009. It received its Slovak registration in 2010, when a new private owner started operating it for the purpose of sports thermal flights. On 29 August 2015, it was damaged extensively in an accident during a field landing. The fuselage and main landing gear structure were severely damaged. According to the preserved photographs and the repair description, the right wing half hit the ground with the end bow and the flap hinge covers of the right wing half were damaged during this occurrence. The only check of the wing surface delamination mentioned in the traced repair documentation was using the tapping test. At that time, the glider had flown 4,308 hrs 28 min and 1,402 flights according to the inspection report from 1 September 2015. The glider was repaired by a service organisation and released into operation. The owner had flown 237 hrs on the glider and performed 74 flights during the operation after the above mentioned repair. In 2020, the third owner was a pilot who did not share the glider with anyone and from 21 July 2021 until 12 August 2023 flew 16 hrs 15 min and made 10 flights.

1.6.4.2 Calculation of the take-off weight of the glider

Weight of an empty glider:	243 kg
Weight of the pilot parachute:	5 kg
Pilot's weight:	80 kg
Total weight of the glider:	328 kg

1.6.4.3 Aerobatic operation:

The first aerobatic flights, which represented a greater load on the glider structure, took place on 25 June 2023 during the Cup of Moravia aerobatic glider competition, when 3 flights were performed with the glider with a total flight time of 45 minutes. On the day of the accident, the glider flew in aerobatic mode for about 10 min and made 1 take-off.

1.6.4.4 Glider maintenance

The annual glider maintenance and airworthiness check was performed on 14 April 2023. The certificate of airworthiness inspection 1045/01/23 was issued with validity until 13 April

2024. No defects have been detected in the glider during its operation since the above actions.

1.7 Meteorological Information

The analysis of the meteorological situation at 12:16 was based on an expert estimate of probable weather at the place of air accident made by the CHMI for the day of 12 August 2023.

The situation:	The weather over the territory of the Czech Republic was under the influence of a cold front from the west, before which warm air was blowing from the south to the territory of the Czech Republic.
Ground wind:	VRB up to 180°/8–10 kt
Upper wind:	2,000 ft AMSL 180° / 10 kt
Visibility:	over 10 km
Weather:	mostly clear with scattered clouds
Cloudiness:	SKC/SCT Cu 2,100–2,400 m
Turbulence:	sporadically weak up to 1,800 m
Ice:	NIL
REG QNH:	1,023 to 1,021 hPa, slight decrease

1.7.1 Abstract from the SYNOP report and extract from the METAR report

Table 2 – Abstract from the SYNOP reports from the meteorological station Čáslav, located approximately 10 km west of the accident site

Time	Visibility [km]	Wind direction	Wind velocity [$m \cdot s^{-1}$]	Wind gusts [$m \cdot s^{-1}$]	Cloud [oktas/m AGL]	Temperature [°C]
12:00	20	130°	4	NIL	2 Ci 7000	30.0
13:00	20	150°	5	NIL	2 Ci 7000	30.0

Table 3 – Extract from the METAR report from the Pardubice airport, located approximately 15 km north-west of the accident site

```
[12.08.2023 13:00Z – 12.08.2023 14:00Z]
METAR LKPD 121300Z 17006KT 100V210 CAVOK 30/12 Q1019 NOSIG RMK BLU BLU=
[12.08.2023 12:30Z – 12.08.2023 13:30Z]
METAR LKPD 121230Z 15006KT 120V200 CAVOK 30/13 Q1019 NOSIG RMK BLU BLU=
[12.08.2023 12:00Z – 12.08.2023 13:00Z]
METAR LKPD 121200Z 17005KT 120V220 CAVOK 29/13 Q1019 NOSIG RMK BLU BLU=
```

1.7.2 Radar, satellite and webcam images

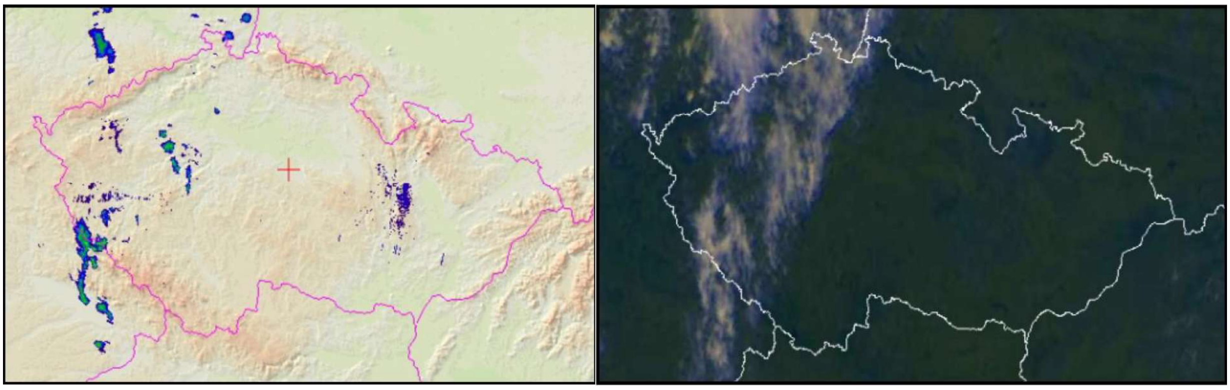

Fig. 6 – Radar and satellite images (the cross indicates the position of the LKPN)

Fig. 7 – Webcam footage from the area of the Seč water reservoir, located approximately 12 km south of the accident site

In the area of the accident near the Podhořany airport, at 12:16, a predominantly south to south-easterly wind of 2 to 4 $m \cdot s^{-1}$ was blowing. Visibility was observed above 10 km, with no dangerous weather phenomena. The sky was almost clear with an occasional high cloud cover. The temperature in the monitored area rose to 30 °C.

1.7.3 Weather from the RADIO controller's diary

The meteorological record at 11:30 CEST shows QNH of 1,019 hPa, the sky almost clear, visibility over 10 km, air temperature 28 °C and wind up to 8 $m \cdot s^{-1}$.

1.8 Radio Navigational and Visual Aids

Visual aids at the LKPN corresponded to the airport category in line with L-14.

1.9 Communications

On the day of the accident, the Providing Information to Known Traffic station at LKPN was activated in accordance with the competition regulations, according to which glider pilots were obliged to communicate with the station on the frequency of 123.590 MHz.

1.10 Airport Information

The Podhořany airport is a public domestic airport with two intersecting grass runways (RWY 07/25 with dimensions 730 × 75 m, RWY 13/31 with dimensions 640 × 92 m). At LKPN, RWY 07 was used for take-off and landing of gliders and was fit for operation. The altitude at the location of the RWY 07 threshold marks is 1,201 ft (366 m). The traffic at the airport had no influence on the occurrence of the air accident.

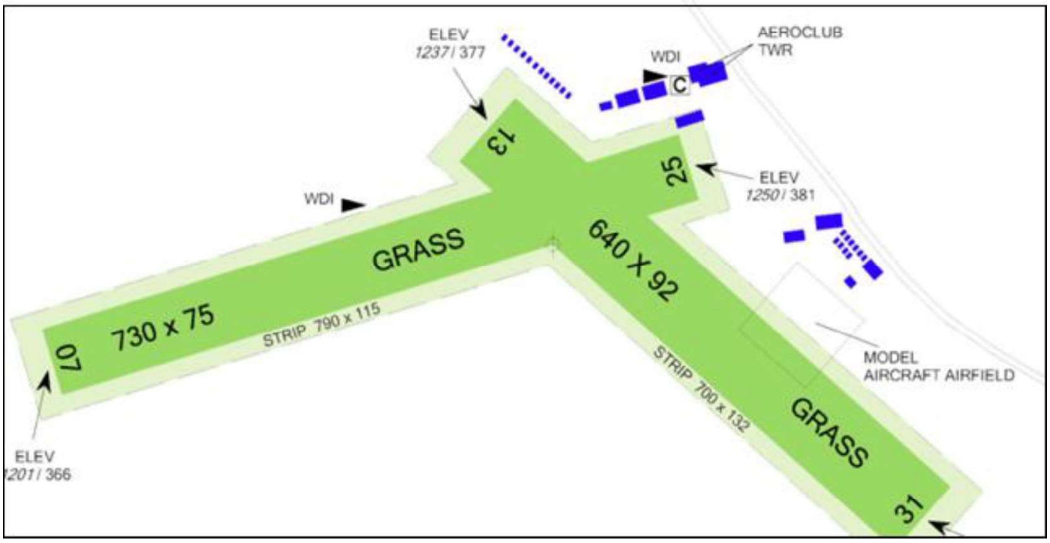

Fig. 8 – Scan of LKPN manoeuvring areas from the VFR manual

1.11 Flight Recorders and Other Means of Recording

No logger, the record of which might be used in the flight analysis, was installed on the glider board.

The competition rules did not require video recording of individual competition flights for the use of the judges.

1.12 Wreckage and Impact Information

The accident site was located on the stubble grain field on the southern outskirts of the village of Podhořany near Ronov, about 150 m south of the junction of the first class road No. 17 and cycle path No. 4179. This is where the glider fuselage, including the tailplanes, was located while the cockpit canopy and the pilot’s emergency parachute were lying in its close proximity, at a distance of about 25 m. The exact location of the glider fuselage impact site is specified in the following table.

Table 4 – Coordinates of the accident site / site of the fuselage and glider tailplanes finding

Geographical coordinates:	N 49°56´01´´
	E 015°31´58´´
Altitude:	277 m

1.12.1 Other Parts of the Glider

The components that separated from the glider fuselage during the flight were found in various parts of the village Podhořany near Ronov. It was the right half of the horizontal tail unit, which was located about 20 m east of the glider fuselage. The right half of the wing was located in a meadow adjacent to cycle path No. 4179 at a distance of approximately 750 m south-west of LKPN RWY 07 threshold marks. The upper part of the left half of the wing skin was found approximately 580 m south-west of the LKPN RWY 07 threshold marks and was driven into the ground with the root end in the area of building plots in the southern part of the village. The left half of the wing was found on the lawn by the road near the garden of house No. 2 at a distance of approximately 470 m west of the LKPN RWY 07 threshold marks. The elevator was subsequently found in the former site of an agricultural cooperative on the south-eastern edge of the village.

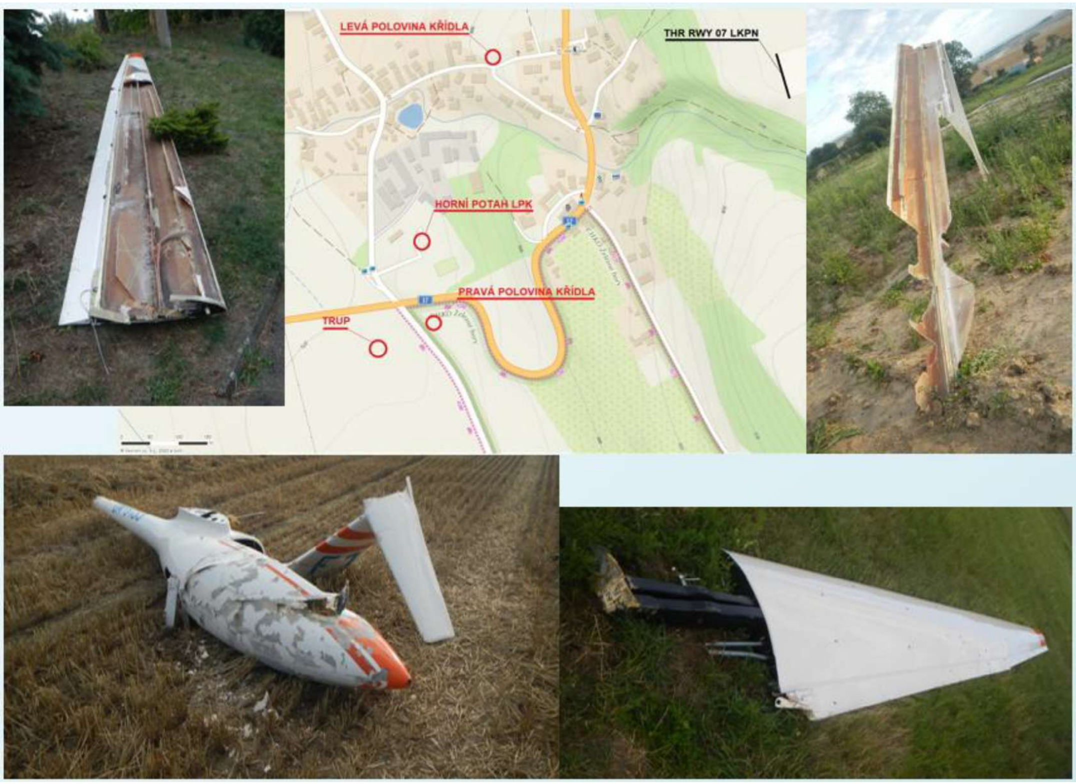

Fig. 9 – Position of the individual parts of the glider wreckage

After the accident site as well as the site where other parts of the glider wreckage had been found were inspected and documented by the Police of the Czech Republic and the AAII inspectors, the wreckage was transported to the depository of the AAII for further examination.

1.12.2 Detailed Inspection of the Wreckage

The glider wreckage was inspected in detail with special attention to both wing halves and their spars, the nature of the damage to both wing halves and their fixing in the fuselage. The Commission invited specialists in laminate and composite structures from Výzkumný a zkušební letecký ústav, a. s. (National Center for Research, Development and Testing in Aerospace) to inspect the critical parts connecting the wing halves.

1.12.2.1 Glider Fuselage

The glider fuselage was completely destroyed when it hit the ground at a steep angle. The right side of the fuselage was torn from the level of the foot controls up to the main landing gear. The lower fuselage was broken in several places. The rear part of the fuselage was cracked longitudinally for about 2 m. Further damage in the form of cracks was on the upper side of the fuselage in the plane where the spars (spar stubs) of both wing halves pass. On the right, there were bent rods for controlling the left aileron and the left aerodynamic brake. There was a noticeable deformation of the front pin bushing. An abrasion mark was visible on the bottom edge of the spar hole (Fig. 10).

Fig. 10 – Left and right fuselage sections profiled to join the wing halves in the root rib plane

1.12.2.2 Cockpit

The cockpit was completely destroyed on impact. The whole front part of the fuselage, especially the lower part, was cracked. The right side of the cockpit was torn away from the plane of the instrument panel towards the rear. The controls were attached to the rods and were deformed. The foot pedals were fitted with metal yokes.

The instrument panel was cracked, but contained all the instruments, including the LUN 1722-8 accelerometer.

Fig. 11 – Glider instrument panel after ground impact

1.12.2.3 Tailplanes

The tailplanes were broken off together with the end part of the fuselage when the glider hit the ground. The elevator by the horizontal tail unit was missing, and was later found approximately 200 m north-west of the fuselage. On the left side of the elevator, there was a crack about 10 cm long. The hinges were mechanically damaged.

1.12.2.4 Wing

The two wing halves were found at a relatively large distance from each other. The left half of the wing was damaged extensively. The upper and lower spar flanges were fractured at the root rib. There were remnants of the root rib of the left half of the wing on the spar stub of the left half of the wing (Fig. 12). The spar web was torn along the length from the root rib to a point about 40 cm from the end bow. The entire upper wing skin, except for the last 40 cm from the end bow, was separated from the left wing structure.

The right half of the wing was damaged to a small extent. On the lower skin of the right half of the wing, there was a crack about 60 cm long at a distance of 120 cm from the outer edge. The left corner of the flap was broken. The spar of the right half of the wing was connected by a pin to the broken spar stub of the left half of the wing (Fig. 13).

Fig. 12 – Remnants of the root rib on the spar of the left half of the wing.

Fig. 13 – Left half of the wing with the remnants of the root rib. An arrow shows the broken lower flange and torn spar web under the upper flange of the spar are shown.

1.13 Search and Rescue

The search was not organised by the RCC. The organiser of the competition sent a car and crew to the site of the presumed wreckage impact. An uninjured pilot was moving near the wreckage, having landed safely on an emergency parachute.

1.14 Tests and Research

Fractographic analysis of the PIK-20D wing spar fracture and Test protocol No.: P-DAV-MTA-123-23 were prepared by VZLÚ, a.s. The subject of the Protocol was an expert assessment of the nature of the fracture areas of the broken spar and determination of the probable mechanism of the fracture of the spar of the left glider wing.

The fractographic analysis of the fracture areas of the damaged wing spar of the glider was performed. The fatigue failure hypothesis was not confirmed because the flange fracture did not show longitudinal separation of individual fibres. Nevertheless, the hypothesis of flange breakage or other damage in the vicinity of the fraction after the previous accident has not been refuted because the fracture contained remnants of the binder from the surface spar layers that may have been deposited there by abrasion from the previous accident. Porosity was observed on the fracture surface of the lower flange and unsaturated fabric on the delaminated layer. Significant porosity was also observed on the sections of the intact parts of both flanges. Porosity has a particular effect on the compressive load capacity of the composite. The observed porosity during the manufacture of the flange could be considered as a permissible defect that was considered when sizing the aircraft. According to the typical strength of the reinforcing fibres used and the macro- and microfractographic signs found, the probable sequence of failure was determined. The wing failure began with a compressive failure of the upper flange with almost immediate subsequent tension fault of the lower flange and subsequent tearing of the fabric overlay between the spar web and the root rib.

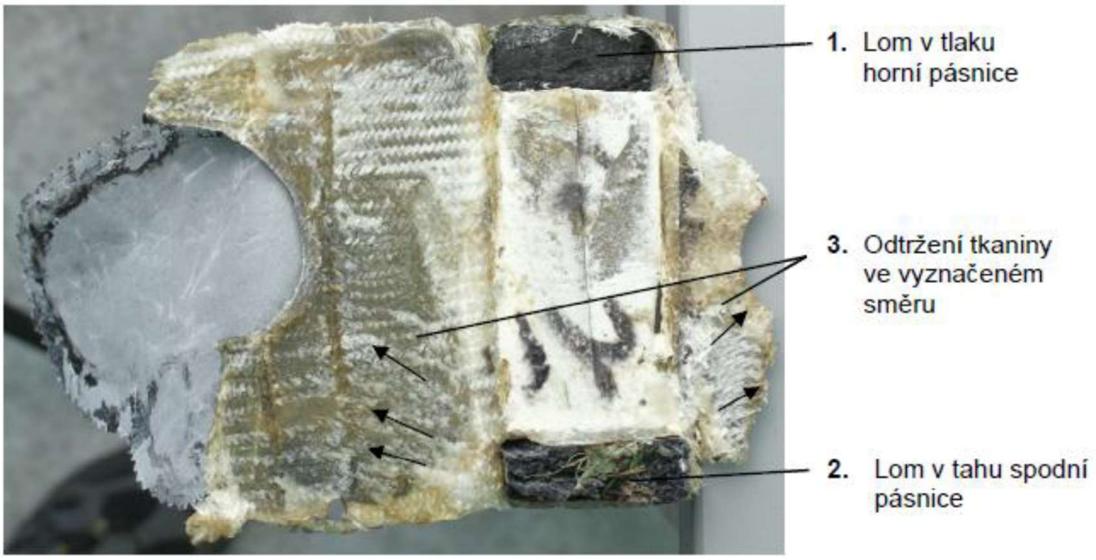

Fig. 14 – Probable sequence of failure of the left wing spar

1.15 Organisational and Management Information

The glider was owned and operated by a natural person and was used for recreational and sports flights.

Participants and organisers of the competition in aerobatics of gliders followed the valid regulations, prepared by the organiser.

1.16 Supplementary Information

1.16.1 PIK-20D Glider Flight Manual, Normal Procedures, 5.7. Aerobatics

PIK-20 D Flight manual

5.6. Cloud flying
— IFR instruments on and monitored
— Air speed within green range
— At air speed exceeding 200 km/h (124 mph, 108 kts) extend the dive brakes
— Observe icing

5.7. Aerobatics
The following aerobatic maneuvers are approved with entry speeds listed below:

Maneuver:	Recommended entry speed		
Steep turn	120 km/h	(75 mph	65 kts)
Looping	185 km/h	(115 mph	100 kts)
Stall turn	170 km/h	(106 mph	92 kts)
Lazy eight	170 km/h	(106 mph	92 kts)
Chandelle	185 km/h	(115 mph	100 kts)
Spin	Use slow deceleration		
Stall (except Whip Stalls)	Use slow deceleration		

Note: Max. entry speed for steep turn, looping, stall turn, lazy eight and chandelle is 190 km/h (118 mph, 103 kts.)

During aerobatic maneuvers monitor accelerometer.

The spin is possible at all C. of G. positions: however in the forward C. of G. position, the sailplane enters a spin with great difficulty. The start of the spin is conventional for sailplanes: Pull control stick fully back and at the same time apply rudder control to the desired direction, then apply full aileron to the same direction. Without aileron control the spin stops after one or two turns. The spin stops by neutralizing the controls. The spin recovers rapidly by applying full rudder opposite to the direction of rotation. Do not push the control stick forward of the neutral position so as to avoid an extreme speed increase. (the loss of altitude is less than 100 m (330 ft))
Note:
Drain the water ballast before aerobatic maneuvers.

EIRIAVION OY
Kisällinkatu 8
SF-15170 Lahti 17

page I-12

Fig. 15 – Scan of page 12 of the Flight Manual

1.16.2 Specific Airworthiness Specification for PIK-20D, Page 6 of 10

Note 6. All PIK-20 D sailplanes are approved for full acrobatic category provided that the following modifications are made.

a) A recording accelerometer with red radials at +6.6 and at -4.6 shall be installed into the sailplane.
b) Foot straps should be installed to the slits existing in the pedals.

1.16.3 Pilot emergency parachute

The glider was equipped with a pilot emergency parachute made by the German manufacturer Brüggemann. It was model 12-82/23R, series P/N 901444-11. The parachute was last repacked by an authorised person in March 2023.

2 Analyses

Majority of facts pointing to the determining of the causes of the air accident arise from the evidence found in the wrecked glider, the findings from the detailed inspection of the air accident location and the location of wreckage, the conclusions of the fractographic analysis of the spar fracture and from the information provided by the witnesses.

2.1 Crew Qualifications

2.1.1 Glider Pilot

The glider pilot had appropriate qualification and valid medical certificate. He had skills in piloting many types of gliders. For the last four years, he has been flying mostly the types ASK-21 and PIK-20D. He started his aerobatic training on 2 May 2019 and obtained the aerobatics-s qualification on 14 October 2019. In 2023, he flew only his own PIK-20D glider and carried out 5 flights lasting 4 hrs 55 min, of which 4 aerobatic ones amounting to 55 min. He performed these aerobatic flights as part of organised aerobatic competitions. On the day of the critical flight, the pilot made one approximately 10-minute flight with the PIK-20D glider. He flew the individual sequence elements without any problems, and despite the unfinished sequence he placed sixth. The pilot confirmed that he was not aware of any moment when he would exceed the permissible load factors by gross interference with the controls and the judges also did not find anything unusual in the execution of the sequence. After the roll, at the moment of transition to the half-loop, the left half of the wing was destroyed and the glider became uncontrollable. The pilot kept his cool and, after jettisoning the cockpit canopy, briefly struggled with unbuckling of the seat belt lock. After unbuckling the seat belts, he was ejected from the glider cockpit by centrifugal force and immediately activated the pilot’s emergency parachute, on which he landed safely in a field near the wreckage. Thanks to his very quick reaction to the critical situation and his mastery of the parachute jump, the pilot did not suffer any injuries during the accident.

2.2 Glider

It had a valid airworthiness certificate and valid statutory liability insurance coverage. The operator maintained the glider in accordance with the relevant requirements. No defects were noted in the maintenance logbook during the previous operation after the annual inspection.

The glider was in an accident in 2015, in which it was damaged to a large extent. The structural integrity of the fuselage was impaired, the main landing gear structure was deformed, both wing halves and rudder were damaged. In September 2015, the glider was repaired and released for operation. As part of the repair, both wing halves were checked for delamination by tapping without any finding. According to records from the glider’s documentation, the glider was not used to fly aerobatic elements from the time of repair until 2023. The glider was used only for thermal overflights and local flights. The critical flight was the fourth flight since the repair in which the glider flew aerobatic elements.

The maximum take-off weight for aerobatic operations was not exceeded. The pilot was not aware of a situation when he would exceed the permissible load factors by interfering with the controls.

The detachment of the upper part of the left wing half, including the rupture of the spar web, occurred during the destruction of the upper and lower spar flanges at the root rib due to dynamic and mechanical forces. The elevator was released from the horizontal tail unit in flight, probably after contact with one of the released wing halves.

The fractographic analysis of the fracture areas of the failed spar confirmed the hypothesis of breakage or other damage in the vicinity of the fractured upper spar flange, probably during the 2015 accident (Fig. 16).

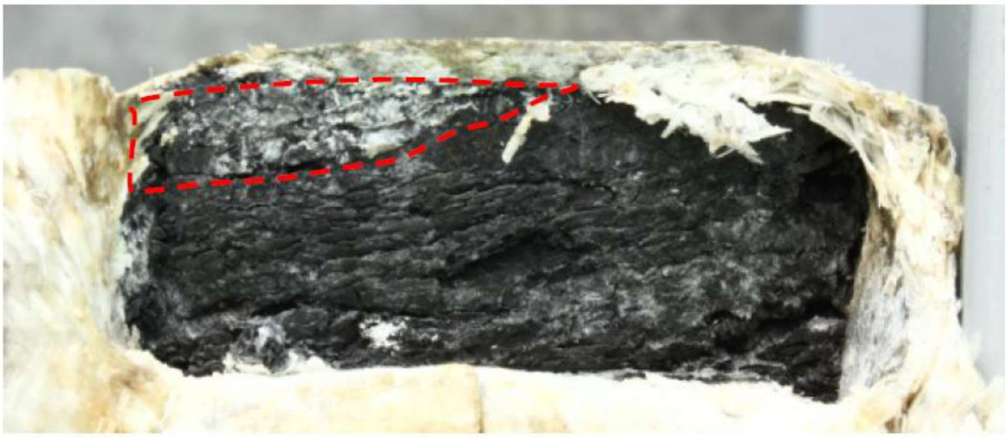

Fig. 16 – Marked failure area at the fracture point of the upper spar flange

Further damage to the glider occurred when the glider hit the ground. The glider hit the ground at a steep angle. The tailplanes were broken off when the aircraft hit the ground. During tailplanes breaking off, control rods caused damage to the fin of the vertical tail unit, ripping the rudder out of its hinges. Also, the right half of the horizontal tail unit was broken off when it hit the ground. The cockpit canopy was destroyed by impact with the ground.

The location and condition of the found wreckage clearly showed that the glider had been destroyed by a breach of structural integrity in flight and only subsequently by the forces applied during the impact on the ground.

2.3 Critical Situation

The critical situation occurred when the pilot, after performing the roll with a subsequent transition to the half-loop, transitioned the glider into a climb by pulling the control stick, which increased the positive g-load factor. The structural integrity of the left half of the wing was compromised as the overload increased. The wing failure began with a compressive failure of the upper flange with almost immediate subsequent tension fault of the lower flange and subsequent tearing of the fabric overlay between the spar web and the root rib and the mechanical destruction of the spar along virtually its entire length, tearing away almost the entire area of the top skin. After the left half of the wing broke off completely, the glider fell to the ground in a left spin. After several turns, the right wing half was spontaneously released from the fuselage. One of the loose wing halves struck the elevator, which broke free from the horizontal tail unit hinges.

The individual parts of the glider luckily just missed the open canopy of the pilot's emergency parachute and did not cause any damage on the ground either.

The glider was not equipped with any recording device from which the flight parameters could be determined and the pilot described the flight as standard. The LUN 1722-8 accelerometer (Fig. 17) recorded the values of -1.0 g and +6.9 g. These values were probably significantly affected by the inertial forces when the fuselage hit the ground and therefore cannot be taken as decisive. The limit values of -4 g and +8 g were probably set by the instrument manufacturer and did not meet the requirements of the PIK-20D Specific Airworthiness Specification document, page 6 of 10, issued by EASA on 27 August 2021.

Fig. 17 – Accelerometer values after the glider hit the ground

2.4 Weather Effects

The synoptic situation during the competition flights met the requirements specified in the aerobatic competition specifications. The maximum ground wind speed was set at 10 m·sec^{-1}.

3 Conclusions

The accident investigation resulted in the following conclusions:

3.1 Findings

3.1.1 Glider Pilot

- held the required and valid licence and was medically fit for performing the given flight,
- has been properly retrained for the type of glider in question,
- the problems with unbuckling seat belts highlighted the need not to underestimate the preparation for dealing with specific cases in emergency situations,
- did not exceed the permissible load factors,
- left the glider in an emergency manner after losing control of the glider,
- activated the pilot's emergency parachute in a timely and correct manner,
- landed safely with his parachute in the field.

3.1.2 Glider

- had a valid certificate of airworthiness inspection and was airworthy,

- had valid liability insurance,
- the overload limits set on the accelerometer did not meet the requirements of the EASA Specific Airworthiness Specification for PIK-20D,
- the destruction of the left wing spar during aerobatic flight was caused by the breakage of the upper spar flange,
- the impairment of structural integrity of the left wing half, the separation of both wing halves from the fuselage and the elevator from the horizontal tail unit occurred in flight,
- the fuselage and tailplanes were destroyed during an impact on the ground.

3.1.3 Meteorological Conditions

- had no effect on the occurrence and progress of the air accident.

3.2 Causes

The cause of the air accident was the destruction of the left wing spar during an aerobatic flight, caused by breakage of the upper spar flange. The failure of the flange was probably caused by the glider’s accident in 2015 and was not identified during the subsequent repair of the glider.

4 Safety Recommendations

During the investigation of the accident CZ-23-0869, a fractographic analysis of the wing spar fracture of the PIK-20D glider revealed that the fracture had occurred in the past, probably during a hard landing in the field. Neither during the post-repair inspection of the glider, nor during other inspections carried out using the approved tapping test method, the failure of the upper wing spar flange has been detected.

4.1 Safety Recommendation CZ-25-0004

Given the cause of the air accident, the Air Accident Investigation Institute recommends that the European Aviation Safety Agency consider conducting a study on the possible use of a more sophisticated methodology for the detection of failures in composite structures to replace the tapping test method used to date.

5 Appendices

Test protocol No.: P-DAV-MTA-123-23 prepared by experts of the Výzkumný a zkušební letecký ústav, a. s. (National Center for Research, Development and Testing in Aerospace)

AEROSPACE P-DMT-LMM-25-003

TEST REPORT

FRACTOGRAPHIC ANALYSIS OF THE PIK-20D WING SPAR FRACTURE

PREPARED BY

Martin Kadlec

APPROVED BY

Petr Homola

Deputy Head of Department

Date of issue of the test report:	10 March 2025
Contract number:	Q15020
Order number:	24/2025
Name of customer:	Ústav pro odborné zjišťování příčin leteckých nehod
Customer contact:	Beranových 130, 199 00 Praha 9 – Letňany
Location of the laboratory activities:	DMT division, LMM department Beranových 130, 199 00 Praha – Letňany
Number of pages including appendix:	12

1. INTRODUCTION

The objective of the report is to perform a fractographic assessment of the fractured spar and to determine the probable fracture mechanism of the spar of the left wing of the PIK-20D glider. The glider had already had a serious accident in the past when the fuselage was severely damaged. For the wing, the repair documentation indicated only an inspection for delamination of the wing skin by tapping. According to the archive photographs, the broken left wing had hit the ground with the end of the wing during this event.

2. DESCRIPTION AND IDENTIFICATION OF SPECIMENS

Date of samples receipt:	5/10/2023
Number of analysed samples:	1

The following damaged left-wing spar part was delivered to the VZLU (Fig. 2.1).

Fig. 2.1 – Provided wing spar part.

3. LIST OF EQUIPMENT

Name	Type	Evidence no.	Additional information
Stereomicroscope	SZ-61	606962	–
Digital microscope	Keyence VHX-6000	V0071100280	–
Ultrasonic cleaner	UC 613HTD	02613424170001	–

4. PROCEDURE AND TEST PARAMETERS

Laboratory activity started on:	01/11/2023
Laboratory activity finished on:	10/11/2023
Analysis performed by:	M. Kadlec, P. Homola, E. Horká

The overview images were taken with a Canon EOS 600D camera. Detailed micrographs were taken using a Keyence VHX-6000 digital microscope with a detachable head at magnifications up to 200x (Fig. 5.1).

Fig. 4.1 – Analysis of fracture with a digital microscope.

5. RESULTS OF ANALYSIS

The overview images of the entire fracture surfaces are shown in Fig. 5.1 to Fig. 5.4. Fig. 5.3a shows the back side of the spar, where the tearing of the fabric occurred when the lower flange was fractured.

Fig. 5.1 – Overview image of the fracture surface from the fuselage view.

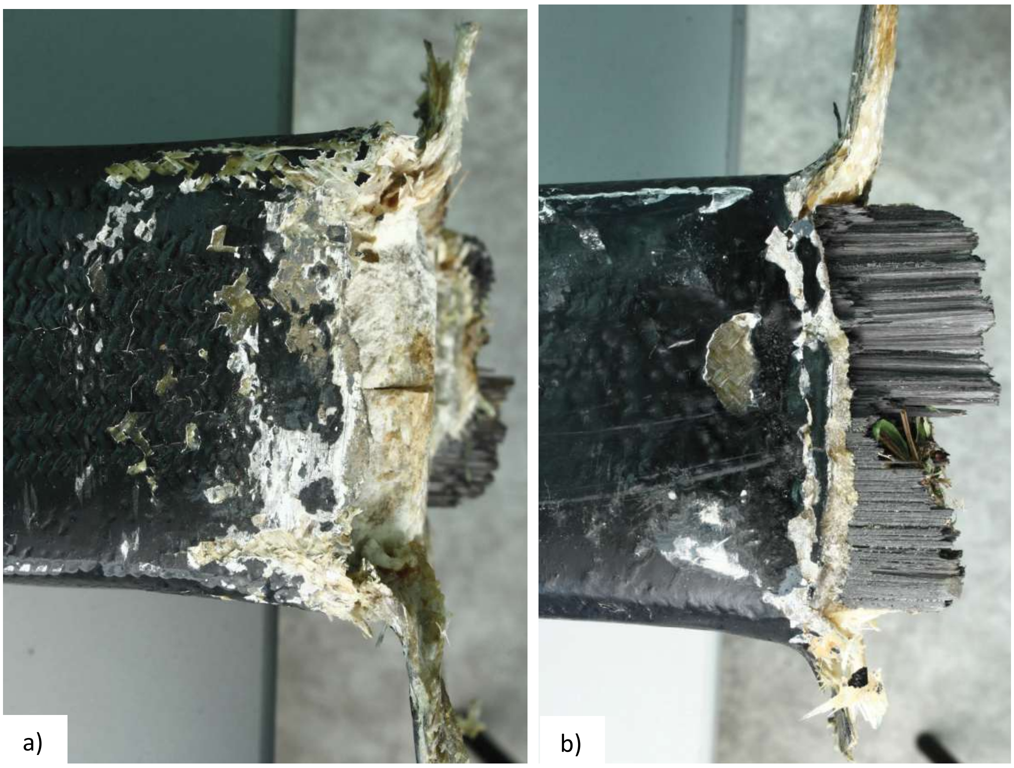

Fig. 5.2 – Overview image of a) upper flange from the top of the spar, b) lower flange from the bottom of the spar.

Fig. 5.3 – Overview image of a) the rear side of the spar, showing the tear in the fabric caused by the fracture of the lower flange, and b) the front side of the spar. The upper flange is always pictured on top.

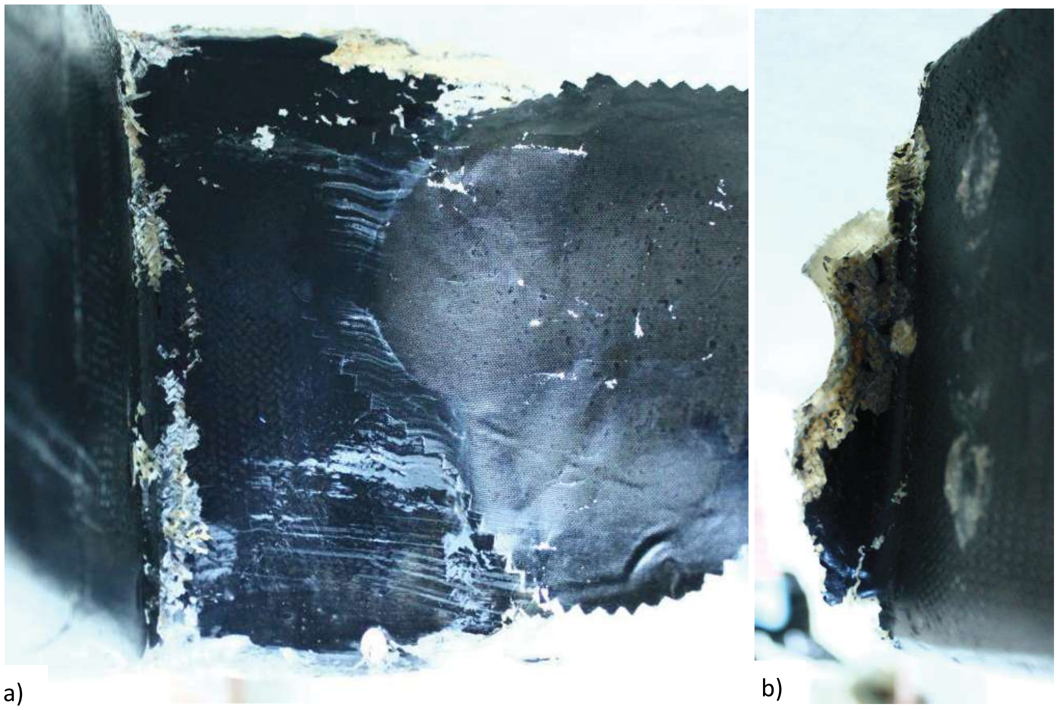

Fig. 5.4 – Overview images of the delaminated fabric on the side of a) the front part and b) the back part. The upper flange is always pictured on top.

The detailed micrographs in Fig. 5.5 show the typical smooth fracture surface caused by the failure of the fibres in compression when the upper flange was subjected to compressive loading. Matrix debris on the fracture surface in compression may indicate fracture in a previous accident, after which the debris from the surface fabric crumbled into the compression fracture surface during service. In contrast, the lower flange shows the typical pull-out fibres caused by tensile stress. The pulled fibre tows do not show the splitting of individual fibres otherwise typical of fatigue failure. It can be deduced that the upper flange was fractured first because typically the compressive strength of the composite is less in compression than in tension.

The detail of the fracture of the upper flange in Fig. 5.6 shows a marked area of matrix debris. Therefore it is suspected to had been fractured in a previous accident.

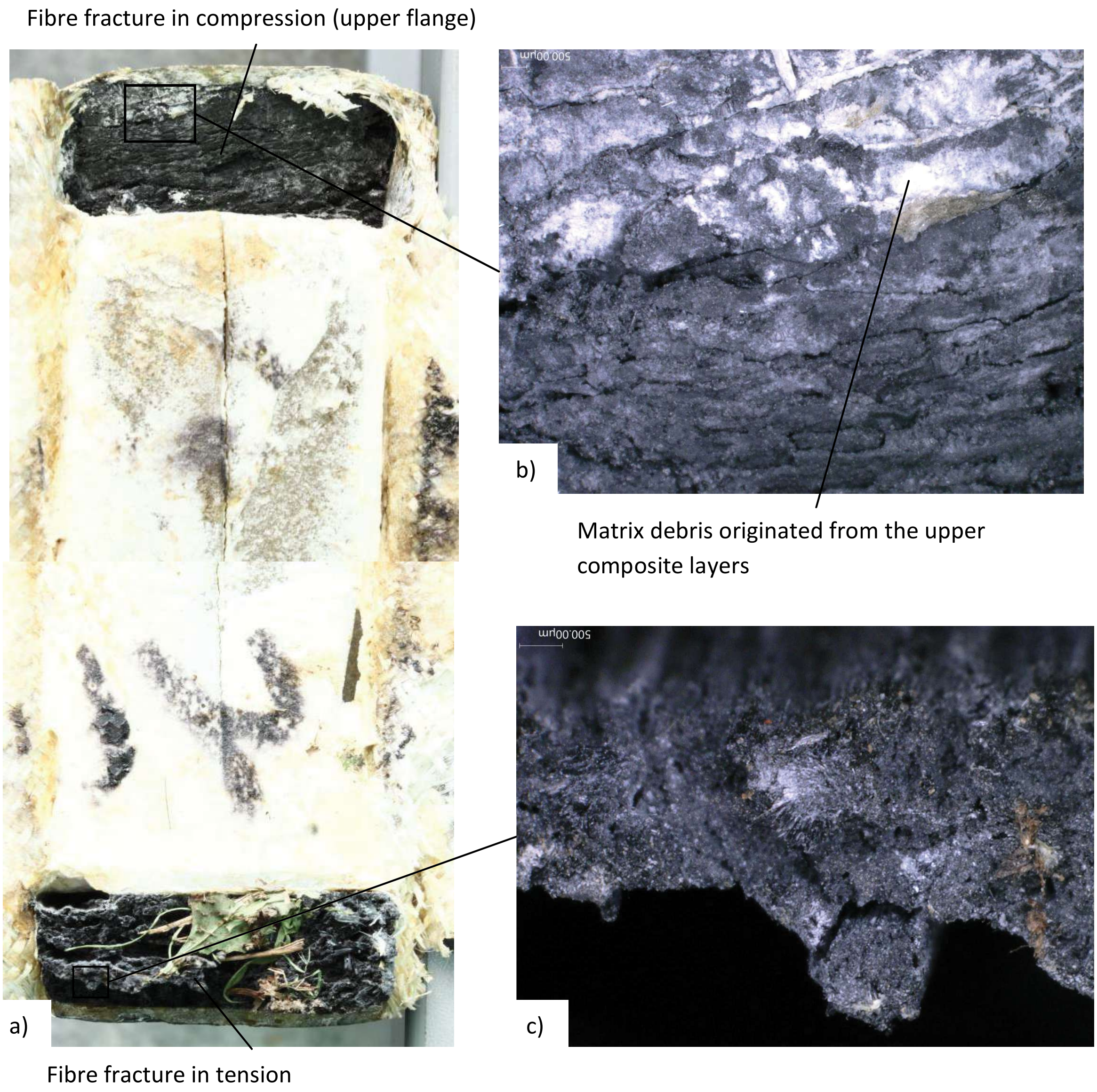

Fig. 5.5 – Overview image with detailed micrographs of carbon fibre fracture, b) detail of the fracture surface of the upper flange fractured in compression with matrix debris from the surface layers, c) detail of the fracture surface of the lower flange fractured in tension.

Fig. 5.6 – Detail of the fractured upper flange with the area suspected to have been fractured in the previous accident. The area contains debris of the matrix from the glass fabric surface layer.

From the detailed micrographs of the fracture surfaces in Fig. 5.7, the following theory of a failure sequence can be confirmed: the glass fabric was torn away after the bottom flange was torn away in tension. This is supported by the river lines in the epoxy that show a local direction of crack propagation from the lower flange, while the overview macrograph shows a radial structure pointing in the same direction. Furthermore, the indentation of the hole at the bottom edge also indicates tearing of the fabric in the direction away from the lower flange. In addition, there was a non-impregnated fabric on the surface of the delaminated composite and black paint residue with fabric impression.

Porosity was evident in the close-up images of the pulled fibre tows of the lower flange. This was observed on both the outer surface at the original interface with the outer fabric (Fig. 5.8) and also on the inner fibre bundles (Fig. 5.9).

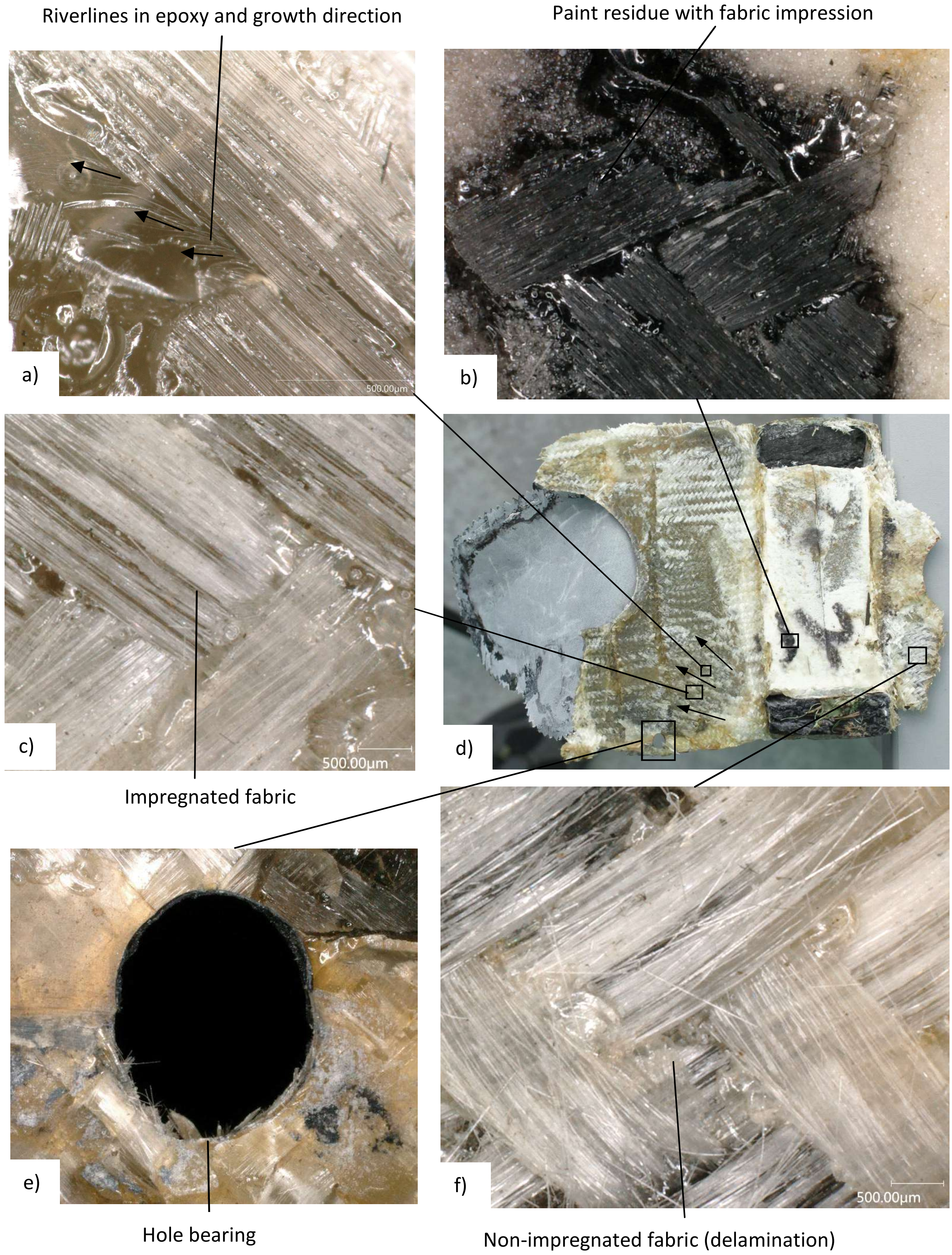

Fig. 5.7 – Marked detailed micrographs of the fracture surface: a) Riverlines in epoxy showing the local direction of crack propagation, b) black paint residue with fabric impression, c) impregnated fibres, d) overview image of the fracture surface with marked radial structure indicating the probable direction of propagation, e) hole bearing at the lower edge indicating fabric tear in the direction from the lower flange, f) non impregnated fabric.

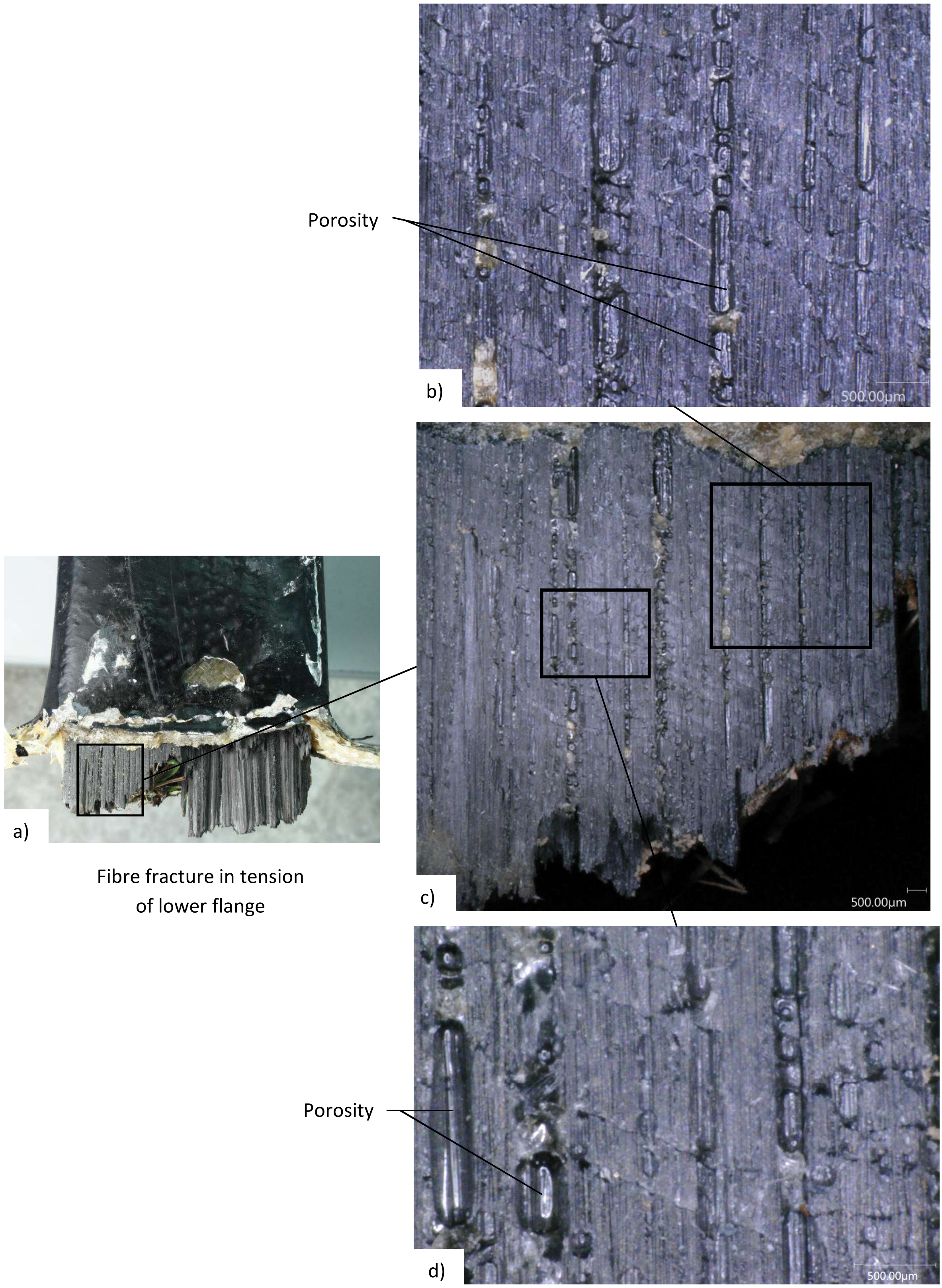

Fig. 5.8 – Overview and details of the outer surface of the fractured lower band with observed porosity.

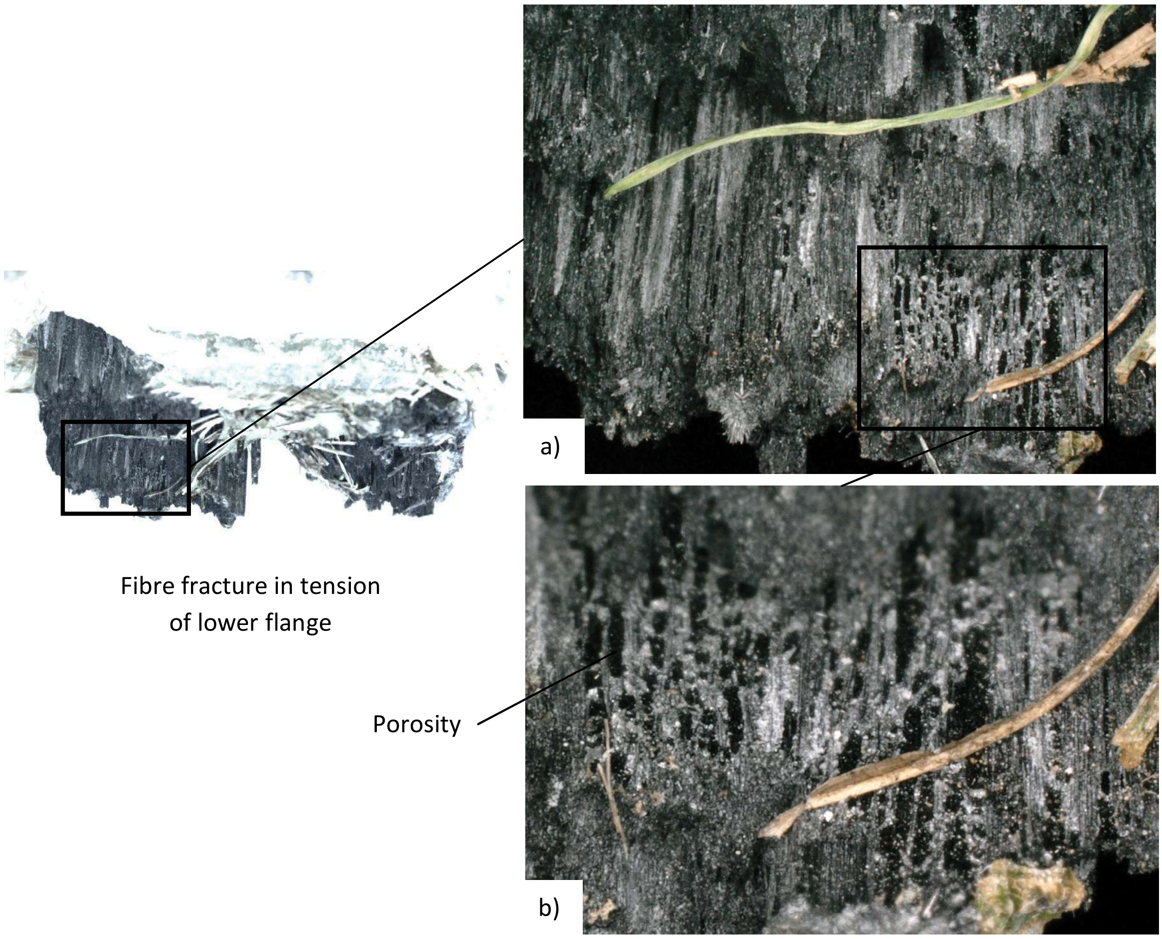

Fig. 5.9 – Overview and details of the internal fracture surface of the lower flange with observed porosity.

Based on the observed porosity in the flange, metallographic analysis of both flanges was carried out at a section approximately 10 cm behind the fracture (Fig. 5.10). In Figs. 5.11 and 5.12, significant porosity is visible on both flanges, particularly at the interface of randomly placed fibre tows. The pore size was 100 to 500 µm. Large pores were also observed at the interface of the inner carbon fibres and the surface fabric, which supported the observed delamination of the fabric at the fracture.

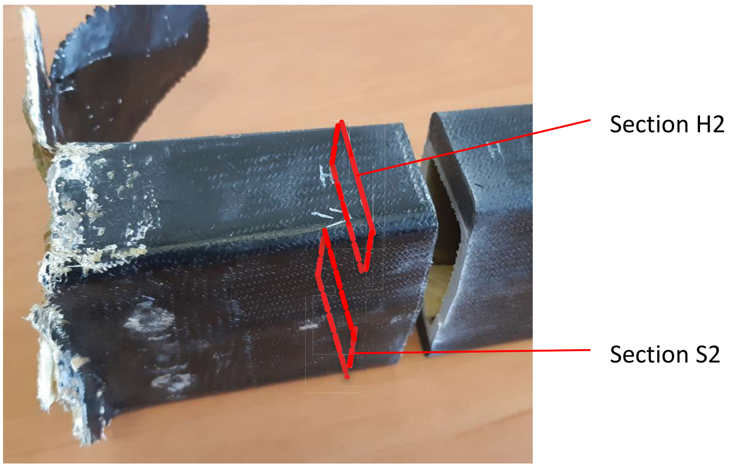

Fig. 5.10 – Schematic representation of sections for metallographic analysis of flange porosity.

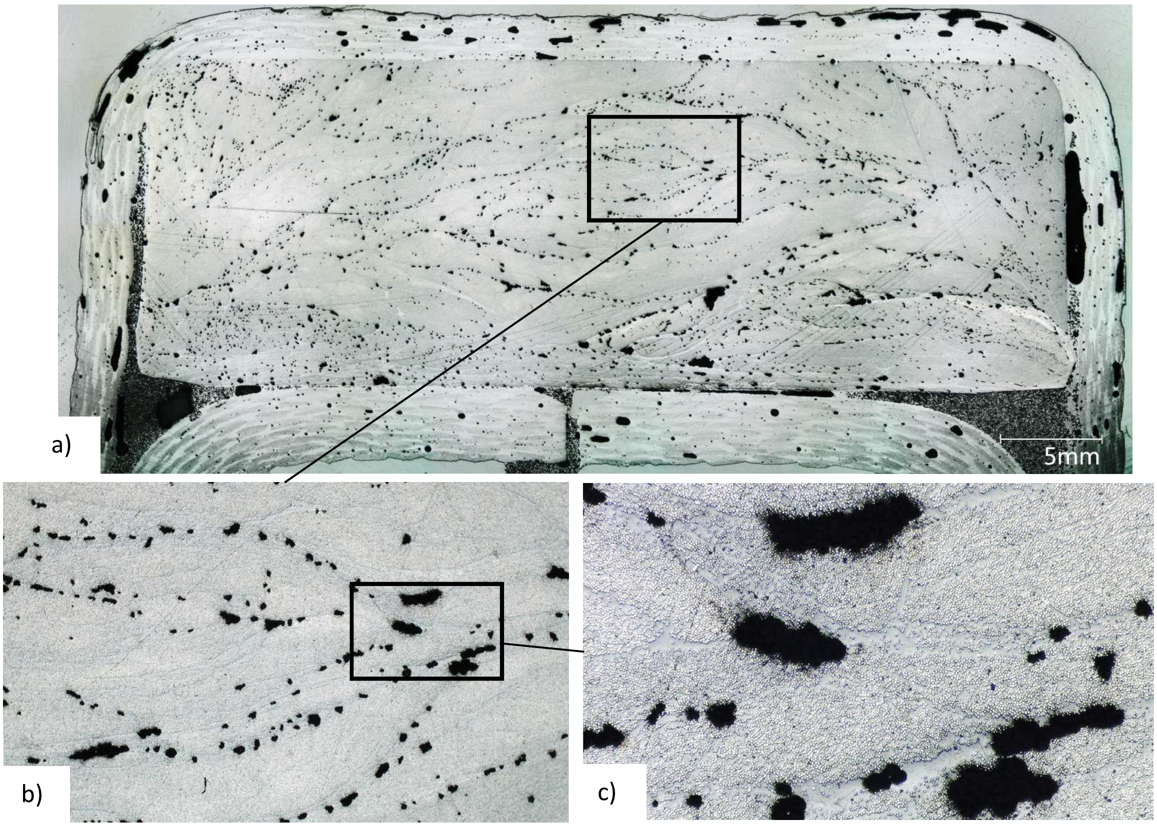

Fig. 5.11 – Section of the upper flange at H2 with significant porosity (black spots) observed: a) Overview image, b) detail at 50x magnification and c) detail at 200x magnification.

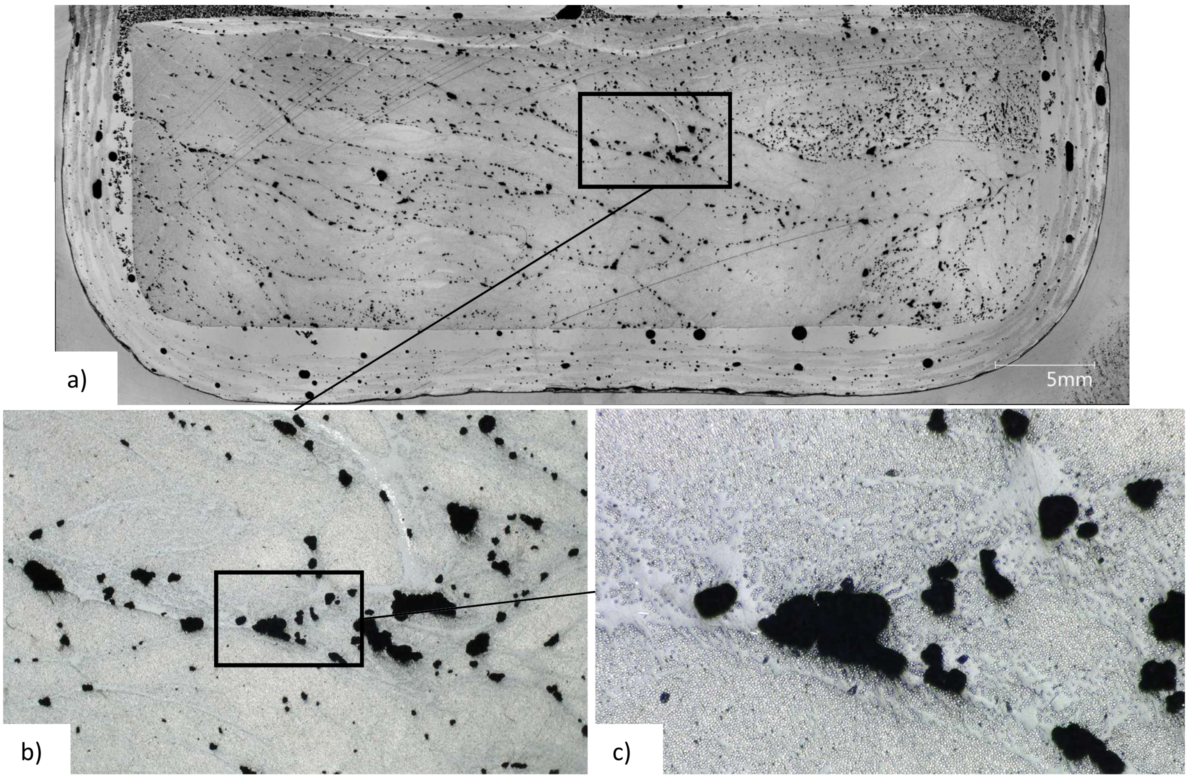

Fig. 5.12 – Section of the lower flange at S2 with significant porosity (black spots) observed: a) Overview image, b) detail at 50x magnification and c) detail at 200x magnification.

6. EVALUATION

Fractographic analysis of the fracture surfaces of the broken wing spar of the PIK-20D glider was performed.

The hypothesis of fatigue failure was not confirmed because the flange fracture does not show longitudinal splitting of individual fibres. However, the hypothesis of flange fracture or existence of other damage in the vicinity of the fracture after the previous accident was not refused because the fracture had matrix debris from the surface layers of the spar that may have been deposited there by abrasion during operation after the previous accident.

Porosity was observed on the fracture surface of the lower flange and non-impregnated fabric on the delaminated layer. Significant porosity was also observed on the sections of the intact sections of both flanges. Porosity has a particular effect on the compressive load capacity of the composite. The observed porosity in the flange manufacture could be considered as an allowable defect that was considered in the aircraft design.

According to the typical strength of the reinforcing fibres used and the macro and micro fractographic features found, a probable failure sequence was determined. The wing failure began with a compressive failure of the upper flange with almost immediate tensile fracture of the lower flange followed by tearing of the fabric overlap between the spar flange and the butt rib (Fig. 6.1).

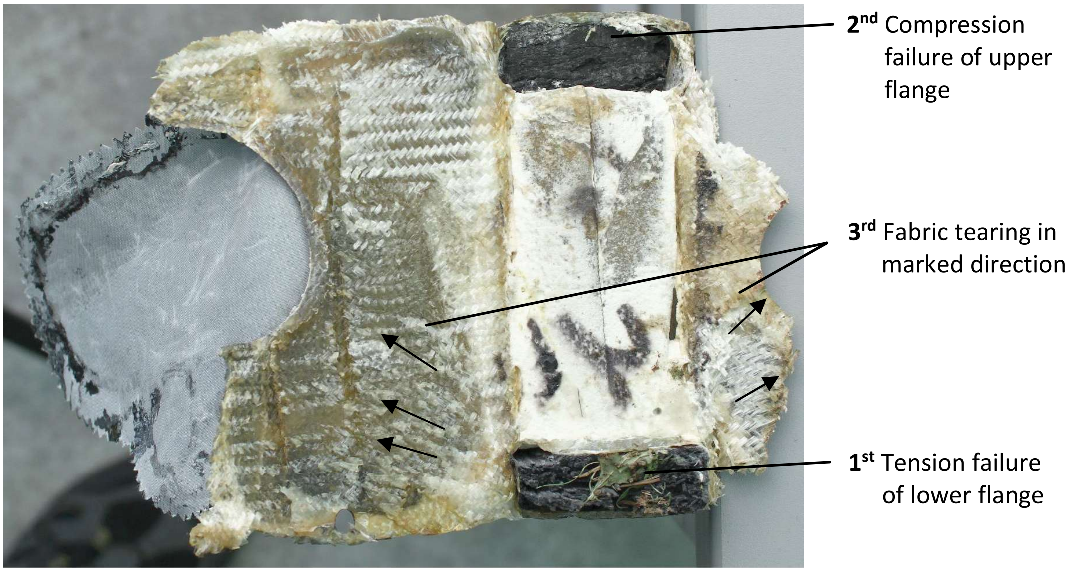

Fig. 6.1 – Probable sequence of the spar failure

7. REFERENCES

Not used.

8. APPENDIX

Not used.

*** END OF TEST REPORT***